CHAPTER 3. TOXICOKINETICS, SUSCEPTIBLE POPULATIONS, BIOMARKERS, CHEMICAL INTERACTIONS

3.1 TOXICOKINETICS

- Absorption of chloroform can occur through the lungs, gastrointestinal tract, and skin.
- Absorbed chloroform is distributed throughout the body. Based on blood-tissue partition coefficients, the equilibrium distribution would be in the following order: fat>>liver>kidney≥ other tissues.
- Chloroform is metabolized by mixed function oxidases (CYP2E1) in the liver, kidney, and other tissues to form reactive intermediates such as phosgene.
- Absorbed chloroform is excreted primarily through the lungs as chloroform. Metabolites are excreted primarily through the lungs as carbon dioxide and in urine to a lesser extent.
- Numerous physiologically based pharmacokinetic (PBPK) models of chloroform have been developed and applied to interspecies and route-to-route dosimetry extrapolation.

3.1.1 Absorption

Inhalation. Absorption of inhaled chloroform depends on many factors, including air concentration, exposure duration, solubility in blood and tissues, and physical activity level, which influences the ventilation rate and cardiac output (Silva et al. 2013). Pulmonary absorption of chloroform is also influenced by total body weight and total fat content, with uptake and storage in adipose tissue increasing with increasing body weight and fat.

Absorption of inhaled chloroform is governed, in part, by its solubility in blood. The blood/air partition coefficient has been estimated in a variety of ways, including experimental measurements made under equilibrium conditions (Batterman et al. 2002; Béliveau and Krishnan 2000a; Gargas et al. 1989; Kaneko et al. 2000) and predictions from physical and/or chemical properties (Abraham et al. 2005; Basak et al. 2004; Poulin and Krishnan 1996). Values from experimental determinations are 7–11 in human blood and 15–21 in rodent blood.

The blood/air partition coefficient has shown concentration dependency when evaluated in rat blood, with values of 16–21 at concentrations <10 µmol (injected into a sealed vial) and 6–9 at concentrations of 37–187 µmol (Béliveau and Krishnan 2000b; Béliveau et al. 2001). Jia et al. (2012) derived a population-based estimate of the blood/air distribution coefficient for chloroform based on data collected on blood

chloroform levels and personal air volatile organic compound (VOC) monitoring in a subset of the 1999–2000 NHANES sample. The blood/air distribution coefficient is a partition coefficient measured under "real-world" conditions, rather than a controlled laboratory setting that cannot account for human variability and often does not evaluate various air concentrations and/or mixed exposure scenarios. Based on NHANES data, the mean distribution coefficient was 51.3 (standard error [SE]=7.0; N=195 adults). This study also found a significant inverse association between the distribution coefficient and the air chloroform concentration, consistent with the experimental data in rat blood.

In inhalation exposures, the arterial blood concentration of chloroform is directly proportional to the concentration in inhaled air. At anesthetic concentrations (8,000–10,000 ppm), steady-state arterial blood concentrations of chloroform were 7–16.2 mg/mL (Smith et al. 1973). Total body equilibrium with inspired chloroform concentration required at least 2 hours at resting ventilation and cardiac output (Smith et al. 1973).

Xu and Weisel (2005) measured blood chloroform kinetics in six adult subjects who inhaled chloroform released from shower water while protected from dermal contact. Observations of air and blood chloroform concentrations were fit to a one-compartment model to estimate an absorption percentage of 71% (range 40–80%).

Aggazzotti et al. (1993, 1995) measured the amount of chloroform absorbed from swimming in indoor swimming pools. Alveolar air samples were collected from both swimmers and observers who did not swim. The chloroform concentration in plasma was correlated with the concentration in air (Spearman's coefficient 0.74). No differences were found between males and females in any exposure group.

Cammann and Hübner (1995) attempted to correlate chloroform exposure with blood and urine chloroform concentrations in persons using indoor swimming pools. Water and air samples were collected from three swimming pools in Germany, with blood and urine samples collected from attendants, normal swimmers, and agonistic swimmers before and after environmental exposure. Pool water chloroform levels ranged from 3.04 to 27.8 µg/L, while air concentrations ranged from 7.77 to 191 µg/m^3. In general, blood chloroform levels increased with exposure. Blood levels were lowest in attendants (0.13–2.45 µg/L), followed by normal swimmers (0.56–1.65 µg/L), and agonistic swimmers (1.14–5.23 µg/L). Based upon the differences seen in the two swimming groups, the study authors concluded that increased physical activity leads to increased absorption and/or ingestion of chloroform.

In a similar study, Lévesque et al. (1994) attempted to quantitate the body burden of chloroform following exposure in an indoor pool. Scuba divers were exposed to chloroform-laden water and air on each of 7 days. On each exposure day, the subjects exercised for a 55-minute period; alveolar air samples were collected before exercise and after 35 or 55 minutes of exercise. Pre-exercise alveolar levels of chloroform averaged 52.6 ppb; this was attributed to air contamination in the locker room. Alveolar air concentrations of chloroform after 35 and 55 minutes of exercise increased steadily through day 5, averaging 0.1–0.95 and 0.104–1.093 ppm, respectively. On day 6, when scuba gear was worn by the subjects, alveolar air concentrations after 35 and 55 minutes of exercise were 0.196 and 0.209 ppm, respectively. The study authors concluded that the average proportions of body burden due to inhalation after 35 and 55 minutes of exercise were 76 and 78%, respectively.

Nashelsky et al. (1995) described one nonfatal assault and three deaths in which chloroform was utilized. Blood and/or tissue concentrations of chloroform were determined in the assault victim and one decedent within 24 hours, within 10 days in another decedent who was frozen for the majority of that period, and after 5 months without preservation in the last decedent. Blood concentrations in two decedents were 2 and 3 µg/mL; fat concentrations were 10 and 42 µg/mL; brain concentrations were 3 and 46 µg/mL; and the liver concentration in one decedent was 24 µg/mL. Due to the nature of the tissues analyzed, these data should be regarded as qualitative indicators of chloroform absorption only.

Yoshida et al. (1999) measured uptake of inhaled chloroform in rats exposed to chloroform in a closed chamber. The kinetics of chloroform uptake from the chamber slowed as the chamber concentration increased from 0.01 to 100 ppm. This observation is consistent with saturable metabolic elimination of absorbed chloroform.

Oral. Peak blood levels were reached 1 hour following ingestion of ^{13}C-labeled chloroform (0.5 g) in a gelatin capsule (Fry et al. 1972). Based on measurements of exhaled chloroform, approximately 100% of the dose was estimated to have been absorbed.

Experiments in mice, rats, and monkeys indicate that oral doses (60 mg/kg) of ^{14}C-labeled chloroform in olive oil were almost completely absorbed as indicated by an 80–96% recovery of radioactivity in expired air, urine, and carcass (Brown et al. 1974a; Taylor et al. 1974). Absorption in mice and monkeys was rapid with peak blood levels reached 1 hour after oral administration of 60 mg/kg chloroform in olive oil.

Studies conducted in mice and rats have found that oral absorption of chloroform is affected by the vehicle in which it is administered. In general, absorption is higher when doses were dissolved in water, compared to corn oil or aqueous 2% Emulphor (Dix et al. 1997; Pereira 1994). Intestinal absorption of chloroform in either water or corn oil administered intragastrically to rats was rapid with both vehicles, but the rate and extent of absorption varied greatly (Withey et al. 1983). The peak concentrations of chloroform in blood were 39.3 µg/mL when administered in water and 5.9 µg/mL when administered in corn oil. The greater degree of absorption following administration in water can be explained by the faster partitioning of a lipophilic compound such as chloroform with mucosal lipids from an aqueous vehicle. Peak blood concentrations were reached somewhat more rapidly with the water vehicle (5.6 minutes as opposed to 6 minutes for corn oil). The uptake from a corn oil solution was more complex (pulsed) than from aqueous solution. A possible explanation for this behavior is that the chloroform in corn oil was broken up into immiscible globules, some of which did not come into contact with the gastric mucosa. Another possible explanation was that intragastric motility may have separated the doses into aliquots that were differentially absorbed from the gastrointestinal tract.

Pereira (1994) investigated the uptake and protein binding of chloroform in the liver and kidney in female B6C3F1 mice. Animals received single doses of chloroform by gavage in either water or corn oil. Uptake of chloroform from water into the liver peaked in 1.5 minutes, and hepatic uptake during the first 20 minutes exceeded that of chloroform delivered in oil. During the first 20 minutes after dosing, binding of chloroform to macromolecules in the liver was greater when water vehicle was utilized; beyond 20 minutes, the amount of binding was equivalent between the two vehicle groups. Renal uptake of chloroform from water exceeded uptake of chloroform from oil over the entire 4-hour period. The extent of binding to macromolecules in kidneys was consistently greater in the group given chloroform in water. Differences in chloroform toxicity based on the vehicle have also been reported elsewhere (Larson et al. 1994b, 1995a).

Dermal. Dermal absorption of chloroform is dependent on ambient temperature. In a study of 10 adult subjects who bathed in water containing 100 µg/L chloroform, the amount of chloroform exhaled when the bath water temperature was 40°C was approximately 40 times that observed when the temperature was 30°C (Gordon et al. 1998). Dick et al. (1995) estimated dermal absorption of chloroform in seven adult subjects. Each subject was exposed to [^{14}C]-chloroform applied to a covered 3.1 cm^2 area of the forearm. The applied doses were 50 µg in water or 250 µg in ethanol and the exposure duration was 8 hours. Absorption was estimated from the sum of ^{14}C exhaled and excreted during a 4-hour period

following the exposure. Mean absorption was 7.8% (standard deviation [SD]=1.4%) when the vehicle was water and 1.6% (SD=0.3%) when the vehicle was ethanol.

Dermal absorption of chloroform is governed, in part, by its rate of diffusion through the skin. Fan et al. (2007) estimated the dermal permeability coefficient (K_P, cm/hour) for chloroform in 11 adult subjects. Each subject was exposed by immersing their hand and forearm in 100 µg chloroform/L water contained in a closed chamber. The K_P was estimated from the rate of change in chloroform concentration in the chamber reservoir. The mean was 0.166 cm/hour (SD: 0.108 cm/hour). In a study in which adult subjects bathed in water containing 40 µg/L chloroform (38°C) while wearing a breathing mask, the K_P, estimated from the rate of chloroform exhaled, was 0.015 cm/hour (Xu and Weisel 2005).

Several studies have estimated the dermal K_P from measurements made in excised human skin preparations. Estimates ranged from 0.016 to 0.16 cm/hour (Dick et al. 1995; Nakai et al. 1999; Poulin and Krishnan 2001; Xu et al. 2002). Differences in estimates may reflect differences in methods used to estimate the K_P (Bunge et al. 1995).

Lévesque et al. (1994) attempted to quantitate the body burden of chloroform following dermal and inhalation exposure in an indoor swimming pool. Male scuba divers were exposed to chloroform-laden water and air on each of 7 days. On each exposure day the subjects exercised for a 55-minute period. On day 6 of the experiment, subjects wore scuba gear to determine the percentage body burden due to dermal exposure. On day 6, when scuba gear was worn by the subjects, alveolar air concentrations after 35 and 55 minutes of exercise were 196 and 209 ppb, respectively. From these data, it would appear that the average proportions of body burden due to dermal exposure after 35 and 55 minutes of exercise were 24 and 22%, respectively.

Cammann and Hübner (1995) attempted to correlate chloroform exposure with blood and urine chloroform concentrations in persons using indoor swimming pools. Water and air samples were collected from three pools in Germany, and blood and urine samples were collected from attendants, normal swimmers, and agonistic swimmers before and after exposure. Pool water chloroform levels ranged from 3.04 to 27.8 µg/L, while air concentrations ranged from 7.77 to 191 µg/m^3. Blood chloroform levels generally increased with higher chloroform exposure levels. Blood levels were lowest in attendants (0.13–2.45 µg/L), followed by normal swimmers (0.56–1.65 µg/L), and agonistic swimmers (1.14–5.23 µg/L). Based upon the differences seen in the two swimming groups, the study authors concluded that increased physical activity leads to increased absorption and/or ingestion. With the

exception of the inclusion of attendants, the study authors did not attempt to differentiate between inhalation and dermal absorption of chloroform. However, the increased blood concentrations seen in the swimmers seems to indicate that dermal absorption did indeed occur.

According to dermal absorption studies with solvents other than chloroform, the absorption of such solvents in guinea pigs is more rapid than metabolism or pulmonary excretion (Jakobson et al. 1982). A dermal absorption rate of 329 nmol/minute/cm^2 (±60 nmol/minute/cm^2) was calculated for the shaved abdominal skin of mice (Tsuruta 1975). This is equivalent to a human absorption rate of 29.7 mg/minute, assuming that a pair of hands are immersed in liquid chloroform (Tsuruta 1975). However, this calculation was based on the assumptions that the rate of chloroform penetration is uniform for all kinds of skin and that the total surface area of a pair of human hands is 800 cm^2; the former assumption is especially dubious.

Islam et al. (1995, 1996, 1999a, 1999b) investigated the fate of topically applied chloroform in male hairless rats. Hairless rats were exposed by immersion in an aqueous solution of chloroform (Islam et al. 1996). Inhalation was prevented by isolating the head in an enclosed chamber. Chloroform was detected in blood within 4 minutes of immersion. Systemic absorption was estimated from the blood chloroform profile (area under the curve [AUC]) observed during and following dermal exposure or an intravenous dose. A 30-minute exposure to 0.44 mg/mL resulted in absorption of approximately 10.2 mg of chloroform. Islam et al. (1999a) estimated absorption of chloroform from dermal exposures to neat chloroform applied to the back of hairless rats. Systemic absorption was estimated from the dermal and intravenous blood chloroform AUC. Rats exposed to 1557 mg chloroform over a 5.46 cm^2 area absorbed approximately 2.8 mg following a 1-minute exposure, 2.5 mg following a 3-minute exposure, and 13.3 mg following an 8-minute exposure. Following cessation of dermal exposure, chloroform was rapidly eliminated from the skin surface by evaporation with a half-time of 2–3 minutes (Islam et al. 1999b). Dermal permeability coefficients (cm/hour) in rats have been estimated from *in vivo* dermal exposure studies (Bogen and Keating 2000).

3.1.2 Distribution

Chloroform is lipid soluble and readily passes through cell membranes, causing narcosis at high concentrations. Blood chloroform concentrations during anesthesia (presumed concentrations 8,000–10,000 ppm) were 7–16.2 mg/mL in 10 patients (Smith et al. 1973). An arterial chloroform concentration of 0.24 mg/mL during anesthesia corresponded to the following partition coefficients: blood/gas, 8;

blood/vessel rich compartment, 1.9; blood/muscle compartment, 1.9; blood/fat compartment, 31; blood/vessel poor compartment, 1; and blood/liver, 2 (Feingold and Holaday 1977). Partition coefficients were calculated for humans based on results in mice and rats, and in human tissues *in vitro*: blood/air, 7.4; liver/air, 17; kidney/air, 11; and fat/air, 280 (Corley et al. 1990).

Tissue/blood partition coefficients for chloroform have been estimated in a variety of ways, including experimental measurements under equilibrium conditions (Gargas et al. 1989; Kaneko et al. 2000; Mahle et al. 2007; Paixao et al. 2013; Thrall et al. 2002) and predictions from physical and/or chemical properties (Abraham and Ibrahim 2006; Abraham et al. 2006; DeJongh et al. 1997; Derricott et al. 2015; Poulin and Krishnan 1996). In general, the highest partition coefficients have been measured in adipose tissue (20–40 times that of other tissues). The value for the tissue/blood partition coefficient depends on the composition of the tissue (Poulin and Krishnan 1996) and varies across species, age, and other factors that affect tissue composition (Mahle et al. 2007).

The chloroform levels in seven patients who died after excessive administration during anesthesia were: brain, 372–480 mg/kg; lungs, 355–485 mg/kg; and liver, 190–275 mg/kg (Gettler and Blume 1931). The chloroform levels in patients under anesthesia who died from other causes were: brain, 120–182 mg/kg; lungs, 92–145 mg/kg; and liver, 65–88 mg/kg tissue wet weight. Nashelsky et al. (1995) described one nonfatal assault and three deaths in which chloroform was utilized. Blood and/or tissue concentrations of chloroform were determined in the assault victim and one decedent within 24 hours, within 10 days in another decedent who was frozen for the majority of that period, and after 5 months without preservation in the last decedent. Blood concentrations in two decedents were 2 and 3 µg/mL; fat concentrations were 10 and 42 µg/mL; brain concentrations were 3 and 46 µg/mL; and the liver concentration in one decedent was 24 µg/mL.

After whole-body autoradiography to study the distribution of ^{14}C-labeled chloroform in mice, most of the radioactivity was found in fat immediately after exposure, while the concentration of radioactivity in the liver increased during the postanesthetic period, most likely due to covalent binding to lipid and protein in the liver (Cohen and Hood 1969). Partition coefficients (tissue/air) for mice and rats were 21.3 and 20.8 for blood; 19.1 and 21.1 for liver; 11 and 11 for kidney; and 242 and 203 for fat, respectively (Corley et al. 1990). Arterial levels of chloroform in mongrel dogs reached 0.35–0.40 mg/mL by the time animals were in deep anesthesia (Chenoweth et al. 1962). Chloroform concentrations in the inhaled stream were not measured, however. After 2.5 hours of deep anesthesia, there was 392 mg/kg chloroform in brain tissue, 1,305 mg/kg in adrenals, 2,820 mg/kg in omental fat, and 290 mg/kg in the liver.

Radioactivity from ^{14}C-labeled chloroform was detected in the placenta and fetuses of mice shortly after inhalation exposure (Danielsson et al. 1986). During early gestation, accumulation of radioactivity was observed in the embryonic neural tissues, while the respiratory epithelium was more involved in chloroform metabolism in the late fetal period.

Due to its lipophilic character, chloroform accumulates to a greater extent in tissues of high lipid content. As shown by the results presented above, the relative concentrations of chloroform in various tissues decreased as follows: adipose tissue > brain > liver > kidney > blood.

No studies were located regarding distribution in humans after oral exposure to chloroform.

Take et al. (2010) compared the distribution of chloroform in rats following separate or simultaneous oral and inhalation exposure. Rats received an oral dose of 55 mg/kg deuterated chloroform ($CDCl_3$) separately or simultaneously with an exposure to 100 ppm chloroform for 360 minutes in a closed chamber. The highest chloroform or $CDCl_3$ concentrations were observed in fat. Combined oral and inhalation exposure increased concentrations of orally administered $CDCl_3$ in blood, fat, kidney, and liver, compared to oral exposure alone. This suggests that the inhaled chloroform altered the disposition of orally administered $CDCl_3$, possibly by inhibiting $CDCl_3$ metabolism.

Take et al. (2014) found that the blood AUC/kg for chloroform following inhalation exposure of rats showed a strong linear correlation (r-0.99) with the inhalation exposure concentration. Based on a linear regression model of inhalation dose and AUC, Take et al. (2014) estimated the inhalation exposure that would be equivalent the AUC/kg observed following oral exposure to chloroform in corn oil. Over the range of oral doses explored (12.5–100 mg/kg), the inhalation equivalent dose ranged from 1.5 to 1.9.

High concentrations of radioactivity were observed in body fat and livers of rats, mice, and squirrel monkeys given oral doses of 60 mg/kg ^{14}C-labeled chloroform (Brown et al. 1974a). The maximum levels of radioactivity in the blood appeared within 1 hour and were 3 µg equivalents chloroform/mL for mice and 10 µg equivalents chloroform/ml for monkeys, which represented ≈0.35 and 1%, respectively, of the total radioactivity. In monkeys, bile concentrations peaked within 6 hours. The distribution of radioactively labeled chloroform was studied in three strains of mice (Taylor et al. 1974). No strain-related differences were observed; however, higher levels of radioactivity were found in the renal cortex of males and in the liver of females. The renal binding of radioactive metabolites may have been altered

by variations in the testosterone levels as a result of hormonal pretreatment in females or castration in males. Sex-linked differences in chloroform distribution were not observed in rats or monkeys (Brown et al. 1974a). Chloroform accumulates in the adipose tissue of rats after oral exposure of intermediate duration (Pfaffenberger et al. 1980).

Islam et al. (1995) investigated the fate of topically applied chloroform in male hairless rats. For exposures <4 minutes, chloroform-laden water was applied to shaved back skin; for exposures of 4–30 minutes, rats were submerged in baths containing chloroform-laden water. Selected skin areas were tape-stripped a various number of times after various delay periods. The study authors found that the accumulated amount of chloroform declined rapidly with depth of stratum corneum. As the time of exposure decreased, smaller amounts of chloroform were found in the deeper layers of stratum corneum; by 5 minutes postexposure, the amount of chloroform at the first tape strip (skin surface) dropped to negligible levels. It appeared that there was an incremental build-up of chloroform in the skin over the first 4 minutes. When compared to uptake measured by bath concentration differences, approximately 88% of the chloroform dose was not accounted for in the stratum corneum and was assumed to be systemically absorbed.

3.1.3 Metabolism

The metabolism of chloroform is well understood. Approximately 50% of an oral dose of 0.5 g chloroform was metabolized to carbon dioxide in humans (Fry et al. 1972). Metabolism was dose-dependent, decreasing with higher exposure. A first-pass effect was observed after oral exposure (Chiou 1975). Approximately 38% of the dose was converted in the liver, and 17% was exhaled unchanged from the lungs before reaching the systemic circulation. *In vivo* metabolic rate constants of $V_{max}C$=15.7 mg/hour/kg and K_M=0.448 mg/L were defined for humans based on pharmacokinetic results obtained from inhalation studies in rats and mice and *in vitro* enzymatic studies in human tissues (Corley et al. 1990). The metabolic activation of chloroform to its toxic intermediate, phosgene, was slower in humans than in rodents.

Metabolic pathways of chloroform biotransformation are shown in Figure 3-1. Metabolism studies indicated that chloroform was, in part, exhaled from the lungs or was converted by oxidative dehydrochlorination of its carbon-hydrogen bond to form phosgene (Pohl et al. 1981; Stevens and Anders 1981). This reaction was mediated by cytochrome P450 and was observed in the liver and kidneys (Ade et al. 1994; Branchflower et al. 1984; Liu et al. 2013; Smith et al. 1984). The dominant isozyme mediating chloroform metabolism in rats and humans is CYP2E1 (Constan et al. 1999; Gemma et al. 2003; Lipscomb et al. 2004; Testai et al. 1996). However, other isoenzymes contribute to the low-affinity phase of oxidative metabolism, including CYP2A6 in humans and CYP2B1/2 in rats (Gemma et al. 2003; Testai et al. 1996). In renal cortex microsomes of DBA/2J mice, the majority of chloroform metabolism was oxidative under ambient oxygen conditions, while anoxic conditions resulted in reductive metabolism (Ade et al. 1994). Phosgene may react with two molecules of GSH to form diglutathionyl dithiocarbonate, which is further metabolized in the kidneys, or it may react with other cellular elements and induce cytotoxicity (Pohl and Gillette 1984). *In vitro* studies indicate that phosgene and other reactive chloroform metabolites bind to lipids and proteins of the endoplasmic reticulum proximate to the cytochrome P450 (Sipes et al. 1977; Wolf et al. 1977). The metabolism of chloroform to reactive metabolites occurs not only in microsomes but also in nuclear preparations (Gomez and Castro 1980). Covalent binding of chloroform to lipids can occur under anaerobic and aerobic conditions, while binding to the protein occurs only under aerobic conditions (Testai et al. 1987).

It was further demonstrated that chloroform can induce lipid peroxidation and inactivation of cytochrome P450 in rat liver microsomes under anaerobic conditions (de Groot and Noll 1989). Covalent binding of chloroform metabolites to microsomal protein *in vitro* was intensified by microsomal enzyme inducers and prevented by GSH (Brown et al. 1974b). It was proposed that the reaction of chloroform metabolites with GSH may act as a detoxifying mechanism. When GSH is depleted, however, the metabolites react with microsomal protein, and may cause necrosis. This is supported by observations that chloroform doses that caused liver GSH depletion produced liver necrosis (Docks and Krishna 1976). In fasted animals, chloroform has been found to be more hepatotoxic (Brown et al. 1974b; Docks and Krishna 1976) even though animals were found to have lower blood chloroform concentrations (Wang et al. 1995); this phenomenon would apparently be explained by a decreased GSH content and resultant inability to bind toxic metabolites. This may explain the clinical finding of severe acute hepatotoxicity in women exposed to chloroform via anesthesia during prolonged parturition. Evidence that chloroform is metabolized at its carbon-hydrogen bond is provided by experiments using the deuterated derivative of chloroform (Branchflower et al. 1984; McCarty et al. 1979; Pohl et al. 1980). Deuterated chloroform was

one-half to one-third as cytotoxic as chloroform, and its conversion to phosgene was much slower. The results confirmed that the toxicity of chloroform is primarily due to its metabolites.

Figure 3-1. Metabolic Pathways of Chloroform Biotransformation

Major aerobic pathway

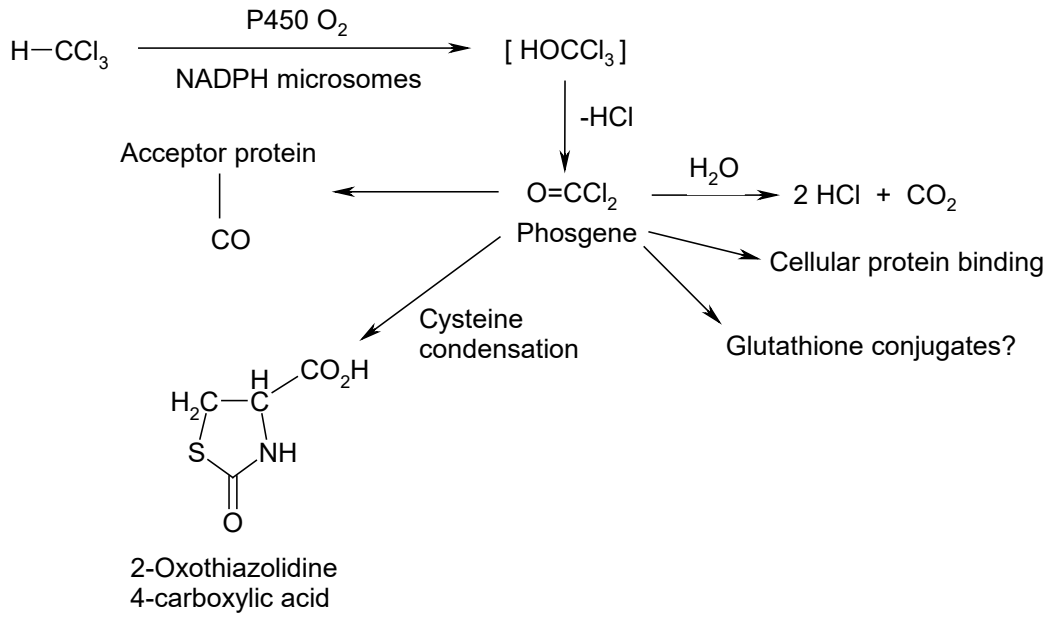

Minor aerobic pathway

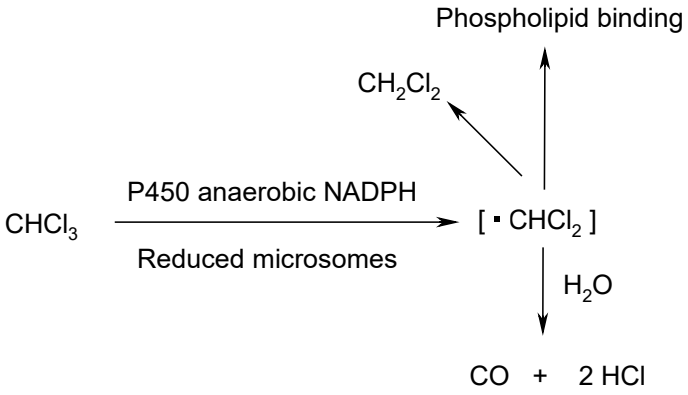

An *in vitro* study of mice hepatic microsomes indicated that a reductive pathway may also play an important role in chloroform hepatotoxicity (Testai et al. 1990, 1995). It was demonstrated that radical chloroform metabolites bind to macromolecules (proteins, lipids) and the process can be inhibited by reduced GSH.

The final product of the aerobic metabolic pathway of chloroform is carbon dioxide (Brown et al. 1974a; Fry et al. 1972). This carbon dioxide is mostly eliminated through the lungs, but some is incorporated into endogenous metabolites and excreted as bicarbonate, urea, methionine, and other amino acids (Brown et al. 1974a). Chloride ions are an end product of chloroform metabolism found in the urine (Van Dyke et al. 1964). Carbon monoxide was a minor product of the anaerobic metabolism of chloroform *in vitro* (Ahmed et al. 1977) and *in vivo* in rats (Anders et al. 1978; Pankow and Damme 1999).

A sex-related difference in chloroform metabolism was observed in mice (Taylor et al. 1974). Chloroform accumulated and metabolized in the renal cortex of males to a greater extent than in females, while liver chloroform concentrations were greater in females than in males; the results may have been influenced by testosterone levels. This effect was not observed in any other species and may explain why male mice were more susceptible to the lethal and renal effects of chloroform than were females (Deringer et al. 1953).

Wang et al. (1994) found that, in male Wistar rats, pretreatment with ethanol increased chloroform metabolism about 2-fold but did not affect hepatic microsomal protein of cytochrome P450 content. In addition, intraperitoneal administration of chloroform resulted in greater blood concentrations, peak values, and AUCs, as compared to oral administration. AUCs in rats administered chloroform orally were 0.34–6.45 versus 0.58–8.78 in rats administered chloroform intraperitoneally. The study authors concluded that differences between route groups in hepatotoxicity were due to differences in the proportion of dose exposed to first-pass metabolism. Since oral dosing results in the greatest first-pass exposure, this route resulted in the greatest hepatotoxicity. The degree of hepatic exposure also influenced the enhancing effect of ethanol; the group receiving chloroform orally was affected the most by ethanol pretreatment. The study authors also concluded that intraperitoneal exposure produced data most like that of inhalation exposure, presumably due to the smaller proportion of dose going through first-pass metabolism.

Interspecies differences in the rate of chloroform conversion were observed in mice, rats, and squirrel monkeys, with species differences in metabolism being highly dependent on dose. The conversion of chloroform to carbon dioxide was highest in mice (80%) and lowest in squirrel monkeys (18%) (Brown et al. 1974a). Similarly, chloroform metabolism was calculated to be slower in humans than in rodents. Therefore, it was estimated that the exposure to equivalent concentrations of chloroform would lead to a

much lower delivered dose in humans (Corley et al. 1990). Inter-strain differences in kinetics of metabolism of chloroform in rodents has also been observed (Vittozzi et al. 2000, 2001).

A study by Gearhart et al. (1993) was conducted to determine the interactions of chloroform exposure with body temperature, gas uptake, and tissue solubility in mice as possible explanations for the difficulty in fitting a physiologically based pharmacokinetic/pharmacodynamic (PBPK/D) model to chloroform gas-uptake data to derive *in vivo* metabolic constants. Male mice were exposed to air concentrations of 100, 800, 2,000, or 5,500 ppm chloroform for 6 hours and their core body temperatures were monitored frequently over the exposure period. After exposure, blood, liver, thigh muscle, and fat tissues were removed for tissue/air and tissue/blood partition coefficient analysis at three temperatures (25, 31, and 37°C). For all tissues, tissue/air partition coefficients exhibited temperature-dependent decreases with increasing temperature. The rate of decrease was greatest for the blood/air partition coefficient. Average body temperatures for each exposure group decreased as the exposure concentrations increased. Temperature-dependent decreases in core body temperature were hypothesized to decrease overall metabolism of chloroform in mice. The data collected were also used to develop a PBPK model for chloroform disposition.

3.1.4 Excretion

Xu and Weisel (2005) measured blood chloroform kinetics in six adult subjects who inhaled chloroform released from shower water while protected from dermal contact with the water. Observations of air and blood chloroform concentrations were fit to a one-compartment model to estimate a residence time (τ) of 13.1 min (±1.62 SD) which corresponds to a first-order half-time of 9.1 minutes ($\tau \cdot \ln[2]$). A two-compartment model fit to the same data yielded half-times of 4.7 and 39 minutes.

Chloroform was detected in the exhaled air of volunteers exposed to a normal environment, heavy automobile traffic, or air in a dry-cleaning establishment (Gordon et al. 1988). Higher chloroform levels in the breath corresponded to higher exposure levels. The calculated biological half-time for chloroform was 7.9 hours.

Following a single, oral exposure, most of the 0.5 g of radioactively labeled chloroform administered to volunteers was exhaled during the first 8 hours after exposure (Fry et al. 1972). A slower rate of pulmonary excretion was observed during the first 8 hours in volunteers who had more adipose tissue than the other volunteers. Up to 68.3% of the dose was excreted unchanged, and up to 50.6% was

excreted as carbon dioxide. A positive correlation was made between pulmonary excretion and blood concentration. Less than 1% of the radioactivity was detected in the urine.

Dick et al. (1995) examined the excretion of chloroform in seven adult subjects following dermal exposure to chloroform. Each subject was exposed to [^{14}C]-chloroform applied to a covered 3.1 cm^2 area of the forearm. The applied doses were 50 μg in water or 250 μg in ethanol and the exposure duration was 8 hours. Urinary excretion of ^{14}C was measured for a period of 3 days following the start of dermal exposure and exhaled ^{14}C was measured for the first 48 hours following the start of exposure. When administered in water, mean urinary excretion was 0.42% of the applied dose and excretion from the lungs was 7.8%. When chloroform was administered in ethanol, the mean urinary excretion was 0.07% of the applied dose and excretion from the lungs was 0.83%

Excretion of radioactivity in mice and rats was monitored for 48 hours following exposure to ^{14}C-labeled chloroform (Corley et al. 1990). In general, 92–99% of the total radioactivity was recovered in mice and 58–98% was recovered in rats; the percentage of recovery decreased with increasing exposure. With increasing concentration, mice exhaled 80–85% of the total radioactivity recovered as ^{14}C-labeled carbon dioxide, 0.4–8% as ^{14}C-labeled chloroform, and 8–11 and 0.6–1.4% as urinary and fecal metabolites, respectively. Rats exhaled 48–85% of the total radioactivity as ^{14}C-labeled carbon dioxide, 2–42% as ^{14}C-labeled chloroform, and 8–11 and 0.1–0.6% in the urine and feces, respectively. A 4-fold increase in exposure concentration was followed by a 50- and 20-fold increase in the amount of exhaled, unmetabolized chloroform in mice and rats, respectively.

Approximately 80% of a single dose of 60 mg/kg ^{14}C-labeled chloroform was converted within 24 hours to ^{14}C-labeled carbon dioxide in mice (Brown et al. 1974a; Taylor et al. 1974), while only ≈66% of the dose was converted to ^{14}C-labeled carbon dioxide in rats (Brown et al. 1974a). Eight hours after administration of 100–150 mg/kg of ^{14}C-labeled chloroform, 49.6 and 6.5% of radioactivity was converted to carbon dioxide, 26.1 and 64.8% was expired as unmetabolized parent compound, and 4.9 and 3.6% was detected in the urine in mice and rats, respectively (Mink et al. 1986). These results indicate that mice metabolize high doses of chloroform to a greater degree than rats. Only 18% of a chloroform dose was metabolized to ^{14}C-labeled carbon dioxide in monkeys, and ≈79% was detected as unchanged parent compound or toluene soluble metabolites (Brown et al. 1974a). Within 48 hours after exposure, ≈2, 8, and 3% of the administered radioactivity was detected in the urine and feces of monkeys, rats, and mice, respectively.

Islam et al. (1996, 1999a) measured the systemic clearance of chloroform in rats following dermal exposures. Elimination of chloroform from blood was biphasic with estimated rate constants (k) of 0.030 and 0.007 minute^{-1} (Islam et al. 1996). The equivalent first-order half-times (ln[2]/k) were 23 and 99 minutes.

3.1.5 Physiologically Based Pharmacokinetic (PBPK)/Pharmacodynamic (PD) Models

PBPK models use mathematical descriptions of the uptake and disposition of chemical substances to quantitatively describe the relationships among critical biological processes (Krishnan et al. 1994). PBPK models are also called biologically based tissue dosimetry models. PBPK models are increasingly used in risk assessments, primarily to predict the concentration of potentially toxic moieties of a chemical that will be delivered to any given target tissue following various combinations of route, dose level, and test species (Clewell and Andersen 1985). Physiologically based pharmacodynamic (PBPD) models use mathematical descriptions of the dose-response function to quantitatively describe the relationship between target tissue dose and toxic endpoints.

3.1.5.1 Summary of PBPK/PD Models

Several rodent and human PBPK models have been used to predict the absorption (oral, inhalation, and dermal) from water and air, distribution, metabolism, and excretion of chloroform (Chinery and Gleason 1993; Corley et al. 1990, 2000; Evans et al. 2020; Gearhart et al. 1993; Haddad et al. 2006; Norman et al. 2008; Reitz et al. 1990; Roy et al. 1996a, 1996b; Sarangapani et al. 2002). Steady-state solutions to chloroform PBPK models for predicting steady-state blood levels have also been reported (Aylward et al. 2010). Some of the above models have been used to support interspecies extrapolation of biologically based dose response models (Conolly and Butterworth 1995; Luke et al. 2010; Pelekis et al. 2001; Sasso et al. 2013; Smith et al. 1995; Tan et al. 2003) or to evaluate the relative contributions of dermal, inhalation, and oral exposure pathways to internal doses of chloroform from environmental exposures such as showering (Haddad et al. 2006; Lyons et al. 2008; Tan et al. 2006, 2007). Population-based models have been developed that account for parameter variability and uncertainty (Delic et al. 2000; Yang et al. 2010).

In a PBPK model that used simulations with mice, rats, and humans (Corley et al. 1990), the tissue delivered dose from equivalent concentrations of chloroform was highest in the mouse, followed by rats, and then humans. The study authors suggested that this behavior is predicted by the model because of the

lower relative rates of metabolism, ventilation, and cardiac output (per kg of body weight) in the larger species. Assuming equivalent target doses produce equivalent toxicities in target tissues, the relative sensitivities of the three species used in the study (mouse > rat > human) predicted by the model under identical exposure conditions are quite different from the relative sensitivity to chloroform assumed by the "uncertainty factor."

In a PBPK/PD model based closely on the Corley model, Reitz et al. (1990) described a pharmacodynamic endpoint (cytotoxicity) in the livers of chloroform-exposed animals produced by phosgene, the reactive metabolite of chloroform.

In gas-uptake experiments, Gearhart et al. (1993) demonstrated a dose-dependent decrease in core body temperature with increased inhaled concentrations of chloroform. The decrease in body temperature could account for decreased *in vivo* chloroform metabolism, partition coefficients, pulmonary ventilation, and cardiac output rates in mice.

Chinery and Gleason (1993) used a shower model for chloroform-contaminated water to predict breath concentration (as a quantifiable function of tissue dose) and actual absorbed dose from a measured water supply concentration following exposure while showering. The model's predictions demonstrated that dose information based only on dermal absorption (without considering an inhalation component) may underestimate actual dose to target organs in dosimetric assessment for chloroform in water supplies during showering. The model also predicted a steady-state stratum corneum permeability of chloroform in human skin in the range of 0.16–0.36 cm/hour, with the most likely value being 0.2 cm/hour. The study authors suggested that the results predicted by this model could be used to estimate household exposures to chloroform or other exposures which include dermal absorption.

McKone (1993) demonstrated that chloroform in shower water had an average effective dermal permeability between 0.16 and 0.42 cm/hour for a 10-minute shower. The model predicted that the ratio of chloroform dermally absorbed in the shower (relative to chloroform-contaminated water concentration) ranged between 0.25 and 0.66 mg per mg/L. In addition, the McKone model demonstrated that chloroform metabolism by the liver was not linear across all dermal/inhalation exposure concentrations and became nonlinear at higher (60–100 mg/L) dose concentrations.

3.1.5.2 Chloroform PBPK Model Comparison

Several chloroform PBPK models that describe the disposition of chloroform in animals and humans have been identified from the open literature (from the early 1980s to 1994). Based on the information presented in these models, there is evidence to suggest that PBPK models for chloroform are fairly refined and have the potential for use in human health risk assessments when key conditions are met (e.g., exposure route and duration, evaluated species, target tissue).

The PBPK model developed by Corley et al. (1990) has provided a basic model for the fate of chloroform in humans and laboratory animals. The Corley et al. (1990) model has been modified in various ways for use in dosimetry extrapolation and exposure pathway apportionment studies (Corley et al. 2000; Delic et al. 2000; Liao et al. 2007; Norman et al. 2008; Roy et al. 1996a, 1996b; Sarangapani et al. 2002; Sasso et al. 2013; Yang et al. 2010). The models of Corley et al. (1990) and Reitz et al. (1990) have described several aspects of chloroform metabolism and disposition in laboratory animals and humans; however, they do not address the dermal routes of exposure.

The models of McKone (1993), Chinery and Gleason (1993), and Corley et al. (2000) address both the inhalation and dermal exposure routes in humans. Several different approaches to modeling the skin have been reported, including single-compartment, well-mixed models (Corley et al. 2000; McKone 1993), multicompartment skin models (Chinery and Gleason 1993; Norman et al. 2008; Roy et al. 1996a, 1996b), and membrane diffusion models (Norman et al. 2008). Further discussion of each model and its application in human risk assessments is presented below.

3.1.5.3 Discussion of Chloroform Models

The Corley et al. (1990, 2000) Model

The Corley model (Corley et al. 1990) was the first chloroform PBPK model to describe and ultimately predict the fate of chloroform in several species (including humans) under a variety of exposure conditions. Many subsequent PBPK models for chloroform are based on the Corley model. Therefore, the Corley model is shown schematically in Figure 3-2 and discussed in-depth below, with subsequent models discussed more briefly. The Corley model has been used for cancer risk assessment (Reitz et al. 1990).

Figure 3-2. Parameters Used in the Corley et al. (1990) Physiologically Based Pharmacokinetic Model

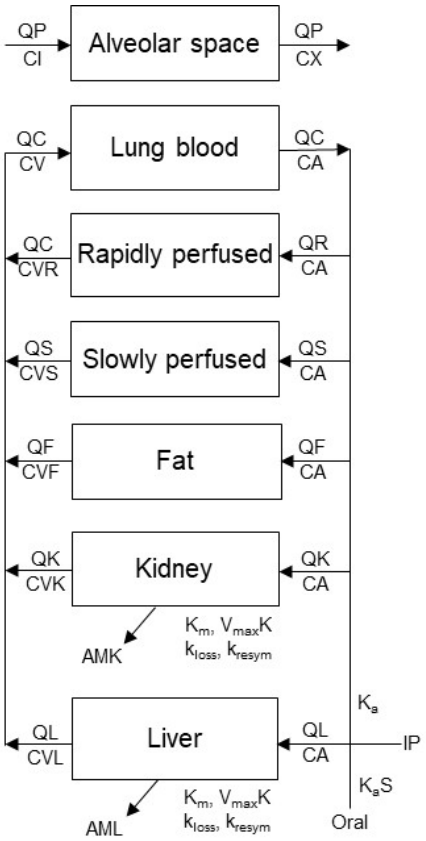

Physiological model used to describe the pharmacokinetics in rats, mice, and humans during inhalation, oral, and intraperitoneal (IP) exposures.

AMK = amount metabolized in kidney; AML = amount metabolized in liver

Risk Assessment. This model successfully described the disposition of chloroform in rats, mice, and humans following various exposure scenarios and developed dose surrogates more closely related to toxicity response. With regard to target tissue dosimetry, the Corley model predicts the relative order of susceptibility to chloroform toxicity to be mouse > rat > human based on macromolecular binding (MMB).

Description of the Model. The Corley chloroform PBPK model was based on an earlier PBPK model developed by Ramsey and Andersen (1984) to describe the disposition of styrene exposure in rats, mice, and humans. A schematic representation of the Corley model (taken from Corley et al. 1990) is shown in Figure 3-2 with oral, inhalation, and intraperitoneal routes represented. Liver and kidney are represented as separate compartments since both are target organs for chloroform. The Corley et al. (1990) model has been modified to include two kidney compartments representing cortex and medulla regions of the kidney

with metabolism assigned to renal cortex and liver (Liao et al. 2007; Sasso et al. 2013). This modification enabled simulation of dosimetry cell death in renal cortex resulting from exposures to chloroform.

The physiologic, biochemical constants and partition coefficients required for the model are shown in Table 3-1. Physiologic constants (organ weight, blood flows, etc.) were similar to those used by Andersen et al. (1987) or were taken from other literature sources. Tissue and blood partition coefficients were determined in tissues by vial equilibration techniques in the rat and human, with extrapolated values used for the mouse. All metabolism of chloroform was assumed to occur only in the liver and kidneys through a single metabolic pathway (mixed function oxidase) that followed simple Michaelis-Menten kinetic parameters. Metabolic rate constants were obtained from the gas uptake experiments. Human metabolic rate constants were obtained from *in vitro* human microsomal fractions of liver and kidney samples using ^{14}C-$CHCl_3$ as the substrate. MMB of chloroform metabolites (phosgene) was assumed to occur in bioactivating tissues (liver and kidney) in a non-enzymatic, nonspecific, and dose-independent fashion. MMB constants for the liver and kidney were estimated from *in vivo* MMB data obtained from rats and mice exposed to ^{14}C-$CHCl_3$ via inhalation.

Table 3-1. Parameters Used in the Corley et al. (1990) Physiologically Based Pharmacokinetic Model

Parameters	Mouse	Rat	Human
		Weights (kg)	
Body	0.02858	0.230	70.0
		Percentage of body weight (%)	
Liver	5.86	2.53	3.14
Kidney	1.70	0.71	0.44
Fat	6.00	6.30	23.10
Rapidly perfused tissues	3.30	4.39	3.27
Slowly perfused tissues	74.14	77.07	61.05
		Flow (L/hour/kg)	
Alveolar ventilation	2.01	5.06	347.9
Cardiac output	2.01	5.06	347.9
		Percentage of cardiac output (%)	
Liver	25.0	25.0	25.0
Kidney	25.0	25.0	25.0
Fat	2.0	5.0	5.0
Rapidly perfused tissues	26.0	26.0	26.0
Slowly perfused tissues	19.0	19.0	19.0

Table 3-1. Parameters Used in the Corley et al. (1990) Physiologically Based Pharmacokinetic Model

Parameters	Mouse	Rat	Human
	Partition coefficients		
Blood/air	21.3	20.8	7.43
Liver/air	19.1	21.1	17.00
Kidney/air	11.0	11.0	11.00
Fat/air	242.0	203.0	280.00
Rapidly perfused/air	19.1	21.2	17.0
Slowly perfused/air	13.0	13.9	12.0
	Metabolic and macromolecular binding constants		
$V_{max}C$ (mg/hour/kg)	22.8	6.8	15.7
K_M (mg/L)	0.352	0.543	0.448
K_{loss} (L/mg)	0.000572	0	0
K_{resyn} ($hour^{-1}$)	0.125	0	0
A (kidney/liver)	0.153	0.052	0.033
fMMB ($hour^{-1}$), liver	0.003	0.00104	0.00202
fMMB ($hour^{-1}$), kidney	0.010	0.0086	0.00931
	Gavage absorption rate constants		
k_{aS} ($hour^{-1}$), corn oil	0.6	0.6	0.6
k_{aS} ($hour^{-1}$), water	5.0	5.0	5.0
	Intraperitoneal injection absorption rate constant		
K_a ($hour^{-1}$)	1.0	1.0	1.0

The gas-uptake data for rats were well described using a single Michaelis-Menten equation to describe metabolism. For the mouse inhalation studies, a simple Michaelis-Menten equation failed to adequately describe the chloroform-metabolizing capacity based on the data collected and model constants. The study authors suspected that, following the administration of chloroform (particularly at higher concentrations), destruction of microsomal enzymes and subsequent resynthesis of microsomal enzymes was important in the mouse. This phenomenon has been documented in phenobarbital-induced rats but not naive rats. To account for this phenomenon, a first-order rate constant for the loss and subsequent regeneration of metabolic capacity was incorporated into the model for mice only.

The model also provided a good description of the *in vivo* levels of MMB in both rats and mice, with good agreement between observed and predicted values.

Corley et al. (2000) expanded the Corley et al. (1990) model to include a skin compartment for simulating dermal exposures. Dermal absorption of chloroform to blood is simulated as a diffusion process governed

by a dermal permeability coefficient (cm/hour), the concentration gradient between the exposure vehicle and skin, a skin/vehicle partition coefficient, and blood flow to the skin. The value for the permeability coefficient was calibrated to data from human studies. In these studies, adult subjects bathed for 30 minutes in an aqueous solution of chloroform while breathing into a face mask to minimize inhalation exposure and to allow measurements of chloroform in exhaled air. The estimated values for the permeability coefficient varied with temperature of the bath. In male subjects, the coefficient decreased from 0.059 cm/hour at 40°C to 0.010 at 30°C. The temperature-related decrease was greater in females compared to males. In the Corley et al. (2000) model the skin is represented as a single well-mixed compartment. Alternatives to this structure have been evaluated. This includes multi-compartment skin models with and without time lags, which attempt to more acutely represent concentration gradients and diffusion rates in various layers of the skin (Norman et al. 2008; Roy et al. 1996a, 1996b). Norman et al. (2008) compared single-compartment and membrane models of dermal absorption of chloroform and concluded that single-compartment, well-mixed models tend to predict faster uptake and lower cumulative uptake than membrane diffusion models or time-lag models.

Sarangapani et al. (2002) developed a modification of Corley et al. (1990) model that included a multicompartment representation of the respiratory tract. The respiratory tract model includes compartments representing the nasal cavity, conducting airways, and pulmonary airways. The nasal cavity and conducting airways have subcompartments representing the lumen, epithelial, and submucosal layers (Morris et al. 1993). Chloroform in the lumen is transferred to the epithelial layer where it can be metabolized or transferred to the submucosa. Absorption to blood occurs from the submucosa. Exchanges between chloroform in air and the epithelial layer are assumed to occur by diffusion, governed by the air-mucus concentration gradient, the mucus surface area, a mass transfer coefficient (cm/hour) and a tissue/air partition coefficient. Absorption of chloroform from the submucosa is assumed to be flow-limited and governed by the concentration gradient between the blood and submucosa and blood flow rate to the respiratory tract region. Metabolism in the epithelial layer is simulated as Michaelis-Menten processes (K_M, V_{max}). Values for tissue/blood partition coefficients and metabolism parameters were derived from various sources (see Table 4 of Sarangapani et al. 2002).

Validation of the Model. The Corley model was validated using chloroform data sets from oral (Brown et al. 1974a) and intraperitoneal (Ilett et al. 1973) routes of administration and from human pharmacokinetic studies (Fry et al. 1972). Metabolic rate constants obtained from the gas-uptake experiments were validated by modeling the disposition of radiolabeled chloroform in mice and rats following inhalation of chloroform at much lower doses. For the oral data set, the model accurately

predicted the total amounts of chloroform metabolized for both rats and mice. After adjustment of the model parameter that describes skin blood flow for the different temperatures and after calibration of the permeability coefficient, the dermal model predicted levels and the temporal pattern of exhaled chloroform in adult subjects who bathed in aqueous solutions of chloroform (90–97 ppb) at temperatures ranging from 30 to 40°C (Corley et al. 2000).

Target Tissues. The model provided excellent predictions of MMB in both the target tissues of chloroform (liver and kidney) after intraperitoneal administration in mice (rat data were not generated). The model adequately predicted the amount of unchanged material exhaled at infinite time and the total amount metabolized by groups of male and female humans of widely varying age and weight.

Species Extrapolation. The Corley model used species-specific information to outline the model parameters; little extrapolation of information among mice, rats, and humans was required. Certain parameters previously reported in the scientific literature were assumed, however, such as body weight, percentage of body weight, and percentage of blood from the heart (i.e., percentage of cardiac output of body organs). The Corley et al. (1990) model has been combined with biologically based dose-response models to predict exposure response relationships in humans (Conolly and Butterworth 1995; Luke et al. 2010; Sasso et al. 2013; Smith et al. 1995; Tan et al. 2003). A sensitivity analysis of the Corley et al. (1990) model examined effects of parameter variability and uncertainty on interspecies extrapolation of internal dose metrics for chloroform (Delic et al. 2000). Yang et al. (2010) derived probability distributions for parameters in the Corley et al. (2000) model that account for population variability and uncertainty.

High-Low Dose Extrapolation. The Corley model was designed to facilitate extrapolations from high doses (similar to those used for chronic rodent studies) to low doses that humans may potentially be exposed to at home or in the workplace.

Inter-route Extrapolation. The Corley model used three routes of administration (intraperitoneal, oral, and inhalation) in rats and mice to describe the disposition of chloroform. These data were validated for humans by comparing the model output using the animal data with actual human data from human oral chloroform pharmacokinetic studies. Using the human pharmacokinetic constants from the *in vitro* studies conducted by Corley, the model made adequate predictions of the amount of chloroform metabolized and exhaled in both males and females. The Corley et al. (2000) model has been applied to

investigate relative contributions of dermal, inhalation, and oral pathways to blood chloroform levels resulting from showering activities (Lyons et al. 2008; Tan et al. 2006, 2007).

The Reitz et al. (1990) Model

Risk Assessment. The Reitz model (Reitz et al. 1990) assumes that cytotoxicity and reparative hyperplasia are responsible for liver neoplasia. Dose surrogates, a more sophisticated and more accurate measure of target tissue dose derived from measuring a pharmacodynamic effect, were used.

Description of the Model. The Reitz et al. (1990) PBPK model was largely based on the Corley et al. (1990) model but differed in the use of a pharmacodynamic end point, cytotoxicity in the livers of chloroform-exposed animals (mice) produced by phosgene (the reactive metabolite of chloroform). The Reitz model focused on the liver as the target organ for chloroform; thus, the kidney compartment toxicity was not addressed. The kidney compartment was combined with the rapidly perfused tissue group. The Reitz et al. (1990) model used two types of dose measurement, referred to as dose surrogates. One type of dose surrogate used was covalent binding to macromolecules, which provided a rate-independent parameter of average daily macromolecular binding (AVEMMB). The second type of dose surrogate was cytotoxicity (PTDEAD), a rate-dependent parameter that measured cell death (by histopathological analysis and ^{3H}thymidine uptake) due to the formation of reactive chloroform metabolites (i.e., phosgene). Model calculations of PTDEAD were based on several assumptions: liver cells have a finite capability for repairing damage caused by chloroform metabolites; liver cells differ from cell to cell in their capabilities to repair this damage; and induction of cytotoxicity in liver cells does not occur instantaneously. A sensitivity analysis of the Reitz et al. (1990) model examined effects of parameter variability and uncertainty on AVEMMB and PTDEAD (Allen et al. 1996). Pelekis et al. (2001) applied the Reitz et al. (1990) model to quantify the uncertainty factor needed to account for differences in internal dosimetry between human adults and children.

Validation of the Model. The model simulations of PTDEAD were compared with two experimental measures of cytotoxicity: the percentage of nonviable cells observed microscopically in mice gavaged with solutions of chloroform in corn oil, and the rate of incorporation of 3H-thymidine into normal DNA during compensatory cell replication (CCR). CCR was measured following exposure of mice to chloroform vapor for 5–6 hours. Model predictions were in good agreement (within 10%) with observed percentages of dead liver cells evaluated microscopically. Agreement between predicted and observed values of cell killing based on CCR was less satisfactory.

Target Tissues. The Reitz model only applies to the metabolism of chloroform and the induction of cytotoxicity in liver tissue following exposure by inhalation, drinking water, and gavage routes using rat and mouse data.

Species Extrapolation. The Reitz model used the same species and physiologic parameters that the Corley model utilized (average body weights, organ percentage of body weight, blood flow, etc.) for model predictions. However, the model assumed equivalent intrinsic sensitivity of mouse and human hepatocytes.

High-Low Dose Extrapolation. The Reitz model was designed to facilitate extrapolations from high doses (similar to those used for chronic rodent studies) to low doses that humans may potentially be exposed to at home or in the workplace.

Inter-route Extrapolation. Inhalation and oral routes of administration were examined in the Reitz model; however, inter-route extrapolations were not specifically addressed in the Reitz model.

The Gearhart et al. (1993) Model

Risk Assessment. The Gearhart et al. (1993) model provided strong evidence that temperature changes play an important role in predicting chloroform metabolism in mice and also provided a testable hypothesis for the lack of fit of the Corley model prediction with respect to the mouse data. These data strengthen the Corley model and its implications for human risk assessment (see the Corley model description above).

Description of the Model. Gearhart et al. (1993) developed a PBPK model that described the effects of decreased core body temperature on the analysis of chloroform metabolic data. Experimental data showed that when male B6C3F1 mice were exposed for 6 hours to chloroform vapor concentrations of 100–5,500 ppm, a dose-dependent drop in core body temperature occurred, with the least amount of temperature drop occurring at the 100-ppm concentration and the most dramatic drop in temperature occurring at the 5,500-ppm level. The Gearhart model incorporated a model previously used by Ramsey and Andersen (1984) (the same model and parameters that the Corley et al. [1990] model was based on) in conjunction with a separate model reflecting changes in body core temperature to drive equations

accounting for changes in partition coefficients, cardiac output, minute ventilation volumes, and rate of chloroform metabolism.

The model predicted that the V_{max} for chloroform metabolism without correcting for core temperature effects was 14.2 mg/hour/kg (2/3 of that reported in the Corley model) and the K_M was 0.25 mg/L. Without body temperature corrections, the model underpredicted the rate of metabolism at the 5,500-ppm vapor concentration. Addition of a first-order kinetic rate constant (kf=1.86 $hour^{-1}$) to account for liver metabolism of chloroform at high doses of chloroform did provide a small improvement in model predictions at 5,500 ppm but was still considered inadequate for predicting metabolism at high concentrations.

Validation of the Model. The Gearhart et al. (1993) model was not validated against a comparable data set. Corrections for the temperature effects (V_{max} increased to 15.1 mg/hour/kg) and inclusion of a first-order metabolism correction equation provided an accurate prediction of chloroform metabolism across all concentrations tested.

Target Tissues. The liver was the target tissue for this model.

Species Extrapolation. No species extrapolation was specifically addressed by the Gearhart et al. (1993) model.

High-Low Dose Extrapolation. No high-low dose extrapolation was specifically addressed by the Gearhart et al. (1993) model.

Inter-route Extrapolation. No inter-route extrapolation was specifically addressed by the Gearhart et al. (1993) model.

The Chinery and Gleason (1993) Model

Risk Assessment. The Chinery and Gleason (1993) model has been applied to estimating exposures to chloroform in a household environment as well as for occupational exposures that result from dermal exposure.

Description of the Model. The Chinery and Gleason (1993) model is a combination of the Corley et al. (1990) model and other existing models that includes a multicompartment skin component similar to that of Shatkin and Szejnwald-Brown (1991). This compartment is used to simulate penetration of chloroform into the skin while showering for 10 minutes with water containing chloroform. The skin module for this new model assumed a physiologic skin compartment consisting of three linear compartments: the dilute aqueous solution compartment; the stratum corneum (the primary barrier to the absorption of most chemicals, including chloroform); and the viable epidermis.

Validation of the Model. The model was validated using published data on experimentally derived exhaled breath concentrations of chloroform following exposure in a shower stall (Jo et al. 1990a).

Target Tissues. Based on the data set of Jo et al. (1990a), the Chinery and Gleason (1993) model predicted the stratum corneum permeability coefficient for chloroform to be 0.2 cm/hour (range 0.6–2.2) and the estimated ratio of the dermally and inhaled absorbed doses to be 0.75 (range 0.6–2.2) cm/hour. This new model showed that a simple steady-state model can be used to predict the degree of dermal absorption for chloroform. It was also shown that the model would be useful in predicting the concentrations of chloroform in shower air and in the exhaled breath of individuals exposed both dermally and by inhalation routes while showering with water containing low amounts (20 μg/L) of chloroform. At this concentration, the model predicted a dermal absorption dose of 0.0047 mg and inhalation absorption dose of 0.0062 mg. In addition, the model also demonstrated that as the concentration of chloroform rises due to increases in chloroform vapor, the absorbed inhalation dose increases faster and becomes larger than the absorbed dermal dose.

Species Extrapolation. No species extrapolation was specifically addressed by this model.

High-Low Dose Extrapolation. No high-low dose extrapolation was specifically addressed by this model.

Inter-route Extrapolation. The Chinery and Gleason (1993) model examined two routes of exposure: inhalation-only exposure and inhalation/dermal exposure. The model was useful in predicting the concentration of chloroform in shower air and in the exhaled breath of individuals exposed by the dermal and inhalation routes.

The McKone (1993) Model

Risk Assessment. The McKone (1993) model has had some use in human chloroform risk assessments, in that the model defined the relationship between the dermal and inhalation exposure to measures of dose and the amounts that can be metabolized by the liver by each route. The model also provided information about the inhalation and dermal exposure concentrations at which chloroform metabolism becomes nonlinear in humans.

Description of the Model. The McKone (1993) model addressed potential exposure to chloroform by the inhalation and dermal routes. McKone (1993) revised existing shower-compartment, dermal uptake, and PBPK models to produce a revised PBPK model for simulating chloroform breath levels in persons exposed in showers by the inhalation route only and by the inhalation and dermal routes combined. Parameters used by this model were taken primarily from two main sources: Jo et al. (1990a) and Corley et al. (1990).

The model was also used to assess the relationship of dermal and inhalation exposure to metabolized dose in the liver, as well as to determine the tap-water concentrations at which hepatic metabolism of dermal and inhalation doses of chloroform become nonlinear. This information is especially useful for risk assessment on persons exposed to a wide range of chloroform concentrations. Experimentally measured ratios of chloroform concentrations in air and breath to tap water concentration (Jo et al. 1990a) were compared with the model predictions.

Validation of the Model. The McKone (1993) model used one data set to evaluate the model results (Jo et al. 1990a). The McKone (1993) model results were also compared to other existing chloroform models, with an in-depth discussion of similarities and differences between those models.

Target Tissues. The skin and lung were the target tissues studied in this model. Based on the information presented, the McKone (1993) model is appropriate for simulating chloroform breath levels in persons exposed in showers by both exposure routes. A major difference between the McKone (1993) model and the Chinery and Gleason (1993) model is that the McKone (1993) model assumes the skin to be a one compartment organ, whereas the Chinery and Gleason (1993) model assumed three compartments within the skin. The McKone (1993) model indicated that the ratio of chloroform dermally absorbed in the shower to the concentration in tap water ranges from 0.25 to 0.66 mg/L, and that

chloroform can effectively permeate through the skin at a rate of 0.16–0.42 cm/hour during a 10-minute shower.

Species Extrapolation. The human was the only species addressed by the McKone (1993) model. No extrapolation between species was addressed in this model.

High-Low Dose Extrapolation. For tap-water concentrations <100 mg/L, the model predicted a linear relationship between potential dose (i.e., amounts present in the drinking water, inhaled in a shower, or skin surface contact) and the cumulative metabolized dose. At tap-water concentrations >100 mg/dL for inhalation-only showers and >60 mg/L for normal showers, however, the relationship was no longer linear and modifications to this model may be required.

Inter-route Extrapolation. The dermal and inhalation routes were addressed in this model. The McKone (1993) model did not specifically address inter-route extrapolations for chloroform.

The Haddad et al. (2006) Model

Description of the Model. The structure of Haddad et al. (2006) PBPK model is similar to that of the Corley et al. (2000) model. The model simulates 6 compartments (lung, liver, fat, skin, richly perfused tissues, poorly perfused tissues) and enables simulations of dermal, inhalation, and oral exposures. All exchanges between blood and tissues are assumed to be flow limited. Metabolism of chloroform is assigned to the liver compartment (K_M, V_{max}). Dermal absorption is simulated with a single well-mixed compartment in which absorption is governed by a dermal permeability coefficient (cm/hour), a skin/vehicle partition coefficient, the concentration difference between the vehicle and skin, and skin blood flow. The dermal permeability coefficient was assigned the value estimated by Xu et al. (2002), which was measured at 25°C. Oral absorption is governed by a bioavailability coefficient (fraction of ingested). Absorption from the lung is assumed to be flow limited and governed by the air concentration, a blood/air partition coefficient, and blood flow to the lung. Values for tissue/blood partition coefficients and metabolism were from various sources (see Table 4 of Haddad et al. 2006). Physiological parameters for adults were from Tardif et al. (1997). These were scaled to age-dependent anthropomorphic data derived from NAHNES III (Price et al. 2003).

Validation of the Model. The model was evaluated against data from human studies in which concentrations of chloroform in exhaled air were measured during dermal exposures from swimming in

an aqueous solution of chloroform (Lévesque et al. 2000). When the permeability coefficient was set to 0.00267 cm/minute (Xu et al. 2002), the predicted blood concentrations were within 1–3 SDs of observed means.

Target Tissues. The Haddad model simulates time-dependent concentrations of chloroform in blood and rates of metabolism of chloroform in the liver. Rates of metabolism could be applied to internal dosimetry of the induction of cytotoxicity in liver tissue following dermal, inhalation, or oral exposures.

Species Extrapolation. Interspecies extrapolations were not investigated in Haddad et al. (2006).

High-Low Dose Extrapolation. High-low dose extrapolations were not investigated in Haddad et al. (2006). Model performance was evaluated at near steady-state concentrations of 10–100 ppb in exhaled air.

Inter-route Extrapolation. The Haddad et al. (2006) model simulates internal doses of chloroform resulting from dermal, inhalation, and oral exposures. The model was used to predict the relative contributions dermal, inhalation, and oral pathways had to blood chloroform levels resulting from showering (Haddad et al. 2006).

The Evans et al. (2020) Model

Description of the Model. Evans et al. (2020) developed a PBPK model of the F344 rat. The structure is similar to that of the Corley et al. (1990) model with the addition of compartments representing the brain and exposure chamber (for simulating closed chamber studies). All exchanges between blood and tissues are assumed to be flow limited. Metabolism of chloroform is assigned to the liver and kidney compartments (K_M, V_{max}). Absorption from the lung is assumed to be flow limited and governed by the air concentration difference, a blood/air partition coefficient, and blood flow to the lung. Values for tissue/blood partition coefficients were measured (see Table 7 of Evans et al. 2020). The values for the metabolism parameters were calibrated to chamber clearance rates measured in closed chamber studies of rats (Evans et al. 2020).

Validation of the Model. The model was evaluated against data from closed chamber studies of rats conducted at starting concentrations ranging from 100 to 3,000 ppm. After calibration of the K_M and V_{max}

parameters, the models precited the time course for the decline in chamber chloroform concentrations (Evans et al. 2020).

Target Tissues. The Evans et al. (2020) model simulates time-dependent concentrations of chloroform in blood and rates of metabolism of chloroform in the liver and kidney. Rates of metabolism could be applied to dosimetry of the induction of cytotoxicity in rat kidney tissues following dermal, inhalation, or oral exposures.

Species Extrapolation. Interspecies extrapolations were not investigated in Evans et al. (2020).

High-Low Dose Extrapolation. Model performance was evaluated at near steady-state initial chamber concentrations ranging from 100 to 3,000 ppm. The model predicted the concentration dependency of chloroform clearance resulting from saturable metabolism of chloroform.

Inter-route Extrapolation. The Evans et al. (2020) model simulates internal doses of chloroform in the F344 rat resulting from inhalation exposures.

3.1.6 Animal-to-Human Extrapolations

Many laboratory animal models have been used to describe the toxicity of chloroform, including rats, mice, rabbits, dogs, and cats (see Tables 2-1, 2-2, and 2-3). By far, rats and mice are the most well-studied laboratory animal species. As discussed in preceding sections of Chapter 3, toxicokinetic data are available from a limited number of human studies, several studies in rats and mice, and a limited number of studies in other laboratory animals (monkeys, guinea pigs). Generally, the pharmacokinetic and toxicokinetic data gathered from rats and mice compare favorably with the limited information available from human studies, with no indication of clear species-related differences that would drastically impact default extrapolation assumptions. PBPK models, such as Corley et al. (2000), have been developed using pharmacokinetic and toxicokinetic data, and some of these have used species-specific information to define model parameters to reduce the amount of extrapolation needed between rodents and humans under some exposure conditions and target tissues (Section 3.1.5). PBPK model conditions, species, and target tissues need to be evaluated for suitability for the selected critical effect prior to use in dose extrapolation for risk assessment in humans.

As mentioned previously, male rodents, particularly mice, have a sex-related tendency to develop severe renal disease when exposed to chloroform, particularly by the inhalation and oral exposure routes. This effect appears to be species-related, since experiments in rabbits and guinea pigs found no sex-related differences in renal toxicity. However, there is no mechanistic data to suggest that the renal disease observed in mice and rats is not relevant to humans.

3.2 CHILDREN AND OTHER POPULATIONS THAT ARE UNUSUALLY SUSCEPTIBLE

This section discusses potential health effects from exposures during the period from conception to maturity at 18 years of age in humans. Potential effects on offspring resulting from exposures of parental germ cells are considered, as well as any indirect effects on the fetus and neonate resulting from maternal exposure during gestation and lactation. Children may be more or less susceptible than adults to health effects from exposure to hazardous substances and the relationship may change with developmental age.

This section also discusses unusually susceptible populations. A susceptible population may exhibit different or enhanced responses to certain chemicals than most persons exposed to the same level of these chemicals in the environment. Factors involved with increased susceptibility may include genetic makeup, age, health and nutritional status, and exposure to other toxic substances (e.g., cigarette smoke). These parameters can reduce detoxification or excretion or compromise organ function.

Populations at greater exposure risk to unusually high exposure levels to chloroform are discussed in Section 5.7, Populations with Potentially High Exposures.

Age and Sex. Numerous animal studies indicate that some male rodents may be more susceptible to the lethal and renal effects of chloroform than female rodents, particularly in mice (Kasai et al. 2002; Larson et al. 1996, 1994b, 1994d; Templin et al. 1996c; Torkelson et al. 1976; Yamamoto et al. 2002). The greater susceptibility of male mice is attributable to increased levels of CYP2E1 activity due to influence of testosterone on CYP2E1 gene transcription (Deringer et al. 1953; Eschenbrenner and Miller 1945; Trevisan et al. 2012). When female mice are co-exposed to androgens and chloroform, renal toxicity was comparable to that observed in exposed males (Culliford and Hewitt 1957; Weir et al. 2005). Conversely, when male mice were castrated, renal toxicity was comparable to that observed in exposed females (Culliford and Hewitt 1957).

Acute lethality studies suggest evidence for age-related susceptibility to chloroform. In acute-duration inhalation lethality studies, young male mice (2 months of age) were slightly susceptible to toxic effects compared to adult mice (Deringer et al. 1953). In rats, acute oral toxicity was similar in young adult and aged animals; however, the LD_{50} value was significantly lower in 14-day-old rats (Kimura et al. 1971).

Pre-existing Conditions, Diseases, and Exposure to Other Substances. Since the liver and kidney are the two main organs responsible for chloroform metabolism, individuals who have hepatic or renal impairment may be more susceptible to chloroform toxicity; one such population would be those who misuse alcohol (Kutob and Plaa 1962; Wang et al. 1994). Also, exhaustion and starvation may potentiate chloroform hepatotoxicity, as indicated in some human clinical reports of women exposed to chloroform as an anesthetic during labor (Royston 1924; Townsend 1939). Chloroform is also more hepatotoxic in fasted animals (Brown et al. 1974b; Docks and Krishna 1976; Ekstrom et al. 1988; McMartin et al. 1981; Wang et al. 1995). These observations are likely due to differential metabolism and detoxification in fasted/starvation states due to fasting-associated induction of hepatic cytochrome P450 enzymes coupled with decreased detoxification capacity due to decreased GSH content (McMartin et al. 1981; Wang et al. 1995).

Obese individuals and those with diseases that lead to fat accumulation in the liver such as alcoholic liver diseases or metabolism associated fatty liver disease may be at increased risk of toxicity since chloroform preferentially distributes to fat (see Section 3.1.2). The kinetics of exposure for lipophilic compounds will be altered in obese individuals, compared to lean individuals. Clearance from blood may be quicker, leading to lower blood levels due to increased uptake in body fat, resulting in an overall extension of half-life and thus increasing cumulative exposure potential (La Merrill and Birnbaum 2011). Increased activity of CYP2E1 has also been observed in obese individuals, especially those with type II diabetes (Brill et al. 2012; Wang et al. 2003), which could also contribute to increased susceptibility to chloroform toxicity in target organs with CYP2E1-mediated effects (e.g., liver and kidney).

Genetic Polymorphisms. Certain genetic polymorphisms may alter the risk of specific cancer types associated with exposure to chlorinated solvents. In a population-based, case-control study assessing women diagnosed with non-Hodgkin's lymphoma, single nucleotide polymorphisms in the DNA repair genes *MGMT* and *NBS1* modified the association between occupational-exposure to chlorinated solvents and increased risk for non-Hodgkin's lymphoma (Jiao et al. 2012). Polymorphisms in the *GSTT1* and *CYP2E1* genes, which are thought to be involved in the metabolism and biotransformation of chloroform,

may increase the risk of childhood acute lymphoblastic leukemia associated with exposure to trihalomethanes in drinking water (Infante-Rivard et al. 2002).

Luzhetskiy et al. (2015) suggested that polymorphisms in the serotonin receptor gene (*HTR2A*) may increase susceptibility to metabolic disorders with exposure to chloroform. Three variations exist, in order of decreasing percent detection: AA, AG, GG. Within the cohort of 212 children assessed, the children with the AG variant showed increased susceptibility to chloroform-associated over-eating and obesity.

3.3 BIOMARKERS OF EXPOSURE AND EFFECT

Biomarkers are broadly defined as indicators signaling events in biologic systems or samples. They have been classified as biomarkers of exposure, biomarkers of effect, and biomarkers of susceptibility (NAS/NRC 1989).

A biomarker of exposure is a xenobiotic substance or its metabolite(s) or the product of an interaction between a xenobiotic agent and some target molecule(s) or cell(s) that is measured within a compartment of an organism (NAS/NRC 1989). The preferred biomarkers of exposure are generally the substance itself, substance-specific metabolites in readily obtainable body fluid(s), or excreta. Biomarkers of exposure to chloroform are discussed in Section 3.3.1. The National Report on Human Exposure to Environmental Chemicals provides an ongoing assessment of the exposure of a generalizable sample of the U.S. population to environmental chemicals using biomonitoring (see http://www.cdc.gov/exposurereport/). If available, biomonitoring data for chloroform from this report are discussed in Section 5.6, General Population Exposure.

Biomarkers of effect are defined as any measurable biochemical, physiologic, or other alteration within an organism that (depending on magnitude) can be recognized as an established or potential health impairment or disease (NAS/NRC 1989). This definition encompasses biochemical or cellular signals of tissue dysfunction (e.g., increased liver enzyme activity or pathologic changes in female genital epithelial cells), as well as physiologic signs of dysfunction such as increased blood pressure or decreased lung capacity. Note that these markers are not often substance specific. They also may not be directly adverse, but can indicate potential health impairment (e.g., DNA adducts). Biomarkers of effect caused by chloroform are discussed in Section 3.3.2.

A biomarker of susceptibility is an indicator of an inherent or acquired limitation of an organism's ability to respond to the challenge of exposure to a specific xenobiotic substance. It can be an intrinsic genetic or other characteristic or a preexisting disease that results in an increase in absorbed dose, a decrease in the biologically effective dose, or a target tissue response. If biomarkers of susceptibility exist, they are discussed in Section 3.2, Children and Other Populations that are Unusually Susceptible.

3.3.1 Biomarkers of Exposure

Chloroform levels can be measured in blood, tissue, urine, breast milk, and expired air; however, levels in blood and expired air have been validated to a higher degree. Since environmental exposure to chloroform likely represents a combination of inhalation (from the air polluted with volatile halogenated hydrocarbons; volatilization from chlorinated water sources), oral (from chlorinated water sources), and dermal (from showering, bathing, or swimming in chlorinated water) exposure routes, interpretation of biomarkers of exposure are challenging. Clewell et al. (2008) reviewed the utility of using a Monte Carlo approach to reconstruct exposure to chloroform from biomonitoring data using blood concentrations of chloroform and validated human PBPK models. They present an exposure conversion factor (ECF) distribution approach to reconstruct likely exposure scenarios via multiroute exposure to estimate chloroform levels in household drinking water. However, this model depends heavily on estimates of background chloroform levels in ambient air, drinking water intake, shower duration and flow rate, and shower stall dimensions. Additionally, the presence of chloroform or its metabolites in biological fluids and tissues needs to be interpreted with caution, as it may reflect exposure to chloroform or the metabolism of other chlorinated hydrocarbons. For example, chloroform also can be detected in the breath after exposure to carbon tetrachloride (CCl_4) and other chlorinated hydrocarbons (Butler 1961).

The relationship between chloroform concentration in inspired air and resulting blood chloroform levels is the most well-defined measure of exposure due to the extensive use of chloroform as a surgical anesthetic. A mean arterial blood concentration of 9.8 mg/dL (range 7–16.6 mg/dL) was observed among 10 patients receiving chloroform anesthesia at an inspired air concentration of 8,000–10,000 ppm (Smith et al. 1973). Monitoring of blood levels in workers experiencing toxic jaundice due to chloroform exposure revealed that when workroom air concentrations were estimated to be >400 ppm, the blood samples of 13 workers with jaundice were 0.10–0.3 µg/l00 mL blood (Phoon et al. 1983). These data suggest an association between increased blood concentrations and increased exposure concentrations, but the blood levels varied too greatly to establish a direct quantitative relationship.

Chloroform is often used as a biomarker for exposure to total trihalomethanes, particularly from chlorinated drinking water and indoor swimming pools. Several studies have examined the increase of chloroform in bodily fluids and/or expired breath as a measure of exposure to trihalomethanes following swimming (Aggazzotti et al. 1995, 1998; Caro and Gallego 2008; Font-Ribera et al. 2010; Pleil and Lindstrom 1997), although these concentrations can vary in swimmers based on their age and physical intensity (Aggazzotti et al. 1995). Correlations have been observed between chloroform concentrations in the air around indoor pools and concentrations in alveolar air (Caro and Gallego 2008; Font-Ribera et al. 2010), and chloroform in alveolar air with concentrations in urine (Font-Ribera et al. 2010). Although chloroform levels in air and water appear to be representative of total trihalomethane exposure (Aggazzotti et al. 1998; King et al. 2004), it has not been proven to be a reliable biomarker of chloroform exposure as elevated tissue levels of chloroform or its metabolites may reflect exposure to other compounds.

3.3.2 Biomarkers of Effect

The primary targets of chloroform toxicity are the CNS, liver, and kidney. The signs and symptoms of CNS effects (e.g., dizziness, fatigue, headache) are easily recognized. Monitoring liver and kidney effects induced by exposure to low levels of chloroform requires the testing of organ functions. Liver effects are commonly detected by monitoring for elevated levels of liver enzymes in the serum or testing for bromosulfalein retention. Urinalysis and measurements of BUN and β-2-microglobin are used to detect abnormalities in kidney function. Because many toxic chemicals can cause adverse liver and kidney effects, these tests are not specific for chloroform. One study attempted to evaluate impaired respiratory health associated with exposure to chlorinated swimming pools using biomarkers of respiratory injury, but no associations were observed with chloroform concentrations in expelled air (Font-Ribera et al. 2010). No specific biomarkers used to characterize effects caused specifically by chloroform were located.

3.4 INTERACTIONS WITH OTHER CHEMICALS

The interactions of chloroform with other chemicals are of particular concern when considering exposure to chlorinated water, which usually contains other trihalomethanes and may contain other potential toxicants. Oral administration of chloroform with one or more trihalomethanes (bromodichloromethane, dibromochloromethane, or bromoform) resulted in higher blood concentrations of chloroform in rats compared to chloroform treatment alone (Da Silva et al. 1999, 2000). Studies on liver and kidney effects

in mice for binary and complex mixtures using four disinfection byproducts (chloroform, bromoform, chlorodibromomethane, bromodichloromethane) suggest that dose-additivity is a reasonable assumption when assessing the toxicity of trihalomethane mixtures (Teuschler et al. 2000).

To further complicate assessment of potential interactions, exposure to disinfection byproducts is often multi-route, including ingestion of tap water as well as dermal and inhalation exposure from showering, bathing, and/or swimming. Florentin et al. (2011) discusses concerns for potential interactions between disinfection byproducts in chlorinated swimming pools, including organohalogens (trihalomethanes, haloacetic acids, halocetonitriles, chloral hydrate, chloropicrin, halophenols, N-chloramines, halofuranones, bromohydrins), non-halogenic organics (aldehydes, alkanic acids, benzene, carboxylic acids), and inorganics (chlorate), and the impact on human health risk assessment. The EPA has developed a cumulative risk assessment model for human exposure to disinfection byproduct mixtures using a cumulative relative potency factors approach, which accounts for both dose and response addition across multiple chemicals via multiple routes (Teuschler et al. 2004). This method groups compounds into subclasses based on common modes of action and selects an index compound for each subclass.

The role that dichloroacetate (DCA) and trichloroacetate (TCA) play in chloroform toxicity was studied in rats (Davis 1992). TCA and DCA are formed in conjunction with chloroform during the chlorination of drinking water; therefore, animals drinking chlorinated water may be exposed to all three compounds simultaneously. It was found that DCA increases the hepatotoxicity and nephrotoxicity of chloroform in rats, that TCA increases the nephrotoxicity of chloroform, and that these effects were gender-specific, occurring mainly in females. Another study found that exposure to chloroform inhibited liver tumor promotion in DCA-treated female mice, while increasing kidney tumor promotion in DCA-treated male mice (Pereira et al. 2001). Combinations of monochloroacetate (MCA) and chloroform toxicity have also shown to have toxic effects on the liver and kidneys of rats (Davis and Bemdt 1992). Additional studies are available that have investigated the mechanisms by which chloroacetic acids (TCA, DCA, MCA) influence the metabolism and metabolic interactions of chloroform and other trihalomethanes (St-Pierre et al. 2003, 2005).

Several animal studies indicate that chloroform can interact with chemicals that induce CYP450 enzymes. The lethal and hepatotoxic effects of chloroform were increased by dicophane (DDT) (McLean 1970) and phenobarbital (a long-acting barbiturate) in rats (Ekstrom et al. 1988; McLean 1970; Scholler 1970). Increased hepatotoxic and nephrotoxic effects were observed after interaction with ketonic solvents and ketonic chemicals in rats (Hewitt and Brown 1984; Hewitt et al. 1990) and in mice (Cianflone et al. 1980;

Hewitt et al. 1979). The hepatotoxicity of chloroform was also enhanced by co-exposure to CCl_4 in rats (Harris et al. 1982), co-exposure to various alcohols (allyl alcohol, methanol, ethanol, isopropanol, t-butanol, pentanol) in rats (Anand et al. 2003; Ray and Mehendale 1990), co-exposure to ethanol in mice (Kutob and Plaa 1962), or co-exposure to chlordecone (Kepone®) in mice and gerbils (Cai and Mehendale 1991; Purushotham et al. 1988). Furthermore, ethanol pretreatment in rats enhanced chloroform-induced hepatotoxicity (Wang et al. 1994) and increased the *in vitro* metabolism of chloroform (Sate et al. 1981).

A series of studies examined the hepatotoxic interaction between chloroform and CCl_4 in rats. Coadministration of chloroform and CCl_4 in ethanol-pretreated rats resulted in dose- and duration-dependent increases in CCl_4-induced hepatotoxicity (Ikatsu and Nakajima 1992). Further studies into the mechanism revealed alterations in ALT and CYP2E1 activity, which only occurred in ethanol-pretreated animals (Ikatsu et al. 1998), suggesting that persons with alcohol use disorder may be a particularly sensitive population to the hepatotoxic effects of chloroform and/or CCl_4 (Lionte 2010).

The potential interaction between chloroform and trichloroethylene has been evaluated with respect to hepatotoxicity in rats (Anand et al. 2005a, 2005b). When administered via intraperitoneal injection, measures of hepatotoxicity (plasma ALT) showed a less-than-additive effect for both compounds. Pharmacokinetic data suggested that chloroform acted in an antagonistic manner with respect to trichloroethylene via inhibition of trichloroethylene metabolism. This relationship was further described in a joint PBPK model for chloroform and trichloroethylene by Isaacs et al. (2004). Since both compounds require bioactivation by CYP2E1 for some toxic effects, less-than-additive toxicity could be explained by mutual inhibition of CYP2E1 metabolism. Based on this logic, other compounds with toxicity mediated via CYP2E1 metabolism may also show interactions with chloroform (e.g., 1,1-dichloroethene; ATSDR 2022a).

Anand et al. (2004, 2005b) proposed that trichloroethylene-induced liver injury was also reduced by co-exposure with chloroform due to increased compensatory liver tissue repair. Several other studies have shown increased compensatory liver tissue repair in rats exposed to binary chemical mixtures of chloroform and other known hepatotoxicants, despite varying mechanisms of toxicity, including allyl alcohol, thioacetamide, and chlordecone (Anand et al. 2003, 2004; Mehendale 1991; Mehendale et al. 1989). As seen in chloroform-only studies (Section 2.9), the capacity for regenerative repair in binary mixture studies resulted in a halted progression of hepatotoxicity and reduction in lethality.

A mixture of cadmium and chloroform potentiated the cytotoxicity of each in *in vitro* experiments in rat hepatocytes (Stacey 1987a, 1987b). In contrast, mirex did not increase chloroform toxicity in mice (Hewitt et al. 1979). Disulfiram, an inhibitor of microsomal enzymes, decreases the hepatotoxicity of chloroform (Masuda and Nakayama 1982; Scholler 1970). Diethyldithiocarbamate and carbon disulfide pretreatment also protect against chloroform hepatotoxicity (Gopinath and Ford 1975; Masuda and Nakayama 1982, 1983), presumably by inhibiting microsomal enzymes. In general, chloroform toxicity can be influenced by chemicals that alter microsomal enzyme activity or hepatic GSH levels. Dimethyl sulfoxide (DMSO) was shown to decrease chloroform-induced hepatotoxicity and nephrotoxicity in male rats, although the mechanism of action has yet to be determined (Lind and Gandolfi 1997; Lind et al. 2000).

Clinical reports of patients who underwent chloroform anesthesia indicated that premedication with morphine caused serious respiratory depression when chloroform was co-administered (Whitaker and Jones 1965). Additionally, thiopentone (thiopental Na, an ultra-short-acting barbiturate anesthetic) was associated with increased incidences of hypotension in chloroform-anesthetized patients (Whitaker and Jones 1965).